Materials for Quantum Technology

OPEN ACCESS

RECEIVED
21 October 2024

REVISED
1 April 2025

ACCEPTED FOR PUBLICATION
10 June 2025

PUBLISHED
24 July 2025

PERSPECTIVE

Bottom-up fabrication of scalable room-temperature diamond quantum computing and sensing technologies

Lachlan Oberg[1,*], **Cedric Weber**[2], **Hung-Hsiang Yang**[3], **Wolfgang M Klesse**[3], **Philipp Reinke**[3], **Santiago Corujeira Gallo**[2,4], **Alastair Stacey**[4,5], **Christopher I Pakes**[6] and **Marcus W Doherty**[1,2]

[1] Department of Quantum Science and Technology, Research School of Physics, Australian National University, Canberra, Australian Capital Territory, 2601, Australia
[2] Quantum Brilliance Pty Ltd, Acton, Australian Capital Territory, 2601, Australia
[3] Quantum Brilliance GmbH, Colorado Tower, Industrietrasse 4, 5.OG 70565 Stuttgart, Germany
[4] School of Science, RMIT University, Melbourne, Victoria, 3000, Australia
[5] Princeton Plasma Physics Laboratory, Princeton University, Princeton, NJ 08540, United States of America
[6] Physics Department, La Trobe University, Melbourne, Victoria, 3086, Australia
[*] Author to whom any correspondence should be addressed.

E-mail: lachlan.oberg@anu.edu.au and marcus.doherty@quantum-brilliance.com

Keywords: NV centre, diamond, quantum computing, quantum sensing, atomically-precise manufacturing, STM, CVD

Abstract

The nitrogen-vacancy (NV) centre in diamond is a premier solid-state defect for quantum information processing and metrology. An integrated diamond quantum device harnesses the collective properties of multiple NV centres, enabling room-temperature quantum computing and sensing. While large-scale devices are poised to fill an important gap in the burgeoning quantum technology landscape, their practical realisation has not been achieved using current top-down fabrication techniques such as ion implantation. Consequently, this necessitates the development of a bottom-up fabrication technique, which is scalable, deterministic, and possesses atomic-scale precision. Informed by existing methods for fabricating phosphorous defect qubits in silicon, we envision a hydrogen depassivation lithography technique for atomically-precise manufacturing of nitrogen-vacancy centres in diamond. This perspective article outlines a viable multi-step procedure for realising scalable fabrication of diamond quantum devices and identifies the key challenges in its development.

The negatively-charged nitrogen-vacancy (NV^-) centre is a point defect in diamond which possesses a unique combination of optical and spin properties [1]. Diamond quantum devices leverage these remarkable properties for compact and room-temperature quantum computation [2, 3] and sensing [4, 5]. This capacity differentiates diamond from leading architectures in the quantum technology landscape, many of which require bulky mainframes or are constrained within dilution fridges. Instead, diamond devices promise to expand the scope of quantum advantage to on-demand computing and sensing in robust operational environments. This vision is embodied through the concept of the *diamond quantum accelerator*; an intermediate-scale quantum computer which seeks to out-compete classical computers of similar size, weight, and power [6]. The ability to widely distribute and integrate quantum accelerators with classical devices offers a potential pathway for long-term adoption in the technological ecosystem. Such devices could be implemented in massively-parallelised quantum computing systems for high-performance computing applications [7–9], and in offline and autonomous systems, such as vehicles, satellites, in medical environments, and for edge computing applications [6, 10].

Unlocking the full capabilities of diamond quantum devices will require a method to fabricate NV centres at scale. This is because the performance of both quantum computers and sensors increases with the number of NV centres integrated within the device. Namely, the qubit volume of a quantum computer scales with the number of entangled defects. While entanglement is not necessarily desirable for conventional quantum sensors, their sensitivity is shot-noise limited and increases with the number of independent defects operating in parallel. However, note that there also exist proposals for enhancing sensitivity through

controlled entanglement schemes [11]. As discussed below, the optimal means for achieving scalability at room-temperature is through an array of closely-spaced and identical NV centres with nanometre-scale separation. Unfortunately, such an architecture cannot be reliably manufactured using existing top-down fabrication techniques, as they do not possess the required spatial resolution or reproducibility. Overcoming this scalability barrier therefore necessitates the development of a bottom-up fabrication process which is both deterministic and possesses sub-nanometre spatial precision. This process is termed atom-scale fabrication [12, 13]. Consequently, the aim of this perspective article is to introduce the major steps involved in the atom-scale fabrication process and to critically consider the key engineering developments necessary for its realisation.

Despite the limitations of current fabrication technology, small scale diamond-based quantum computing is already an existing reality [2, 14–16]. The pivotal element of these computing devices is the quantum processing node, comprised of an NV^- centre (consisting of a substitutional N atom adjacent to a vacancy) surrounded by a cluster of nearby nuclear spins (typically ^{13}C nuclei). The nuclear spins act as the qubits of the computer, whilst the NV^- centre mediates qubit initialisation, readout, and intra-node multi-qubit operations. Quantum computation is then controlled via radiofrequency, microwave, optical and magnetic fields. Each processing node contains at minimum one qubit, realised through the nuclear spin of the N which composes the NV itself. Whilst the number of qubits can be increased through the presence of nearby ^{13}C spins, a single NV centre can control at most 5–10 qubits; beyond this point, the nuclear hyperfine levels of the satellite spins cannot be resolved spectrally. Existing devices are therefore limited by small qubit volumes.

Scaling a diamond quantum computer will therefore require fabrication of many quantum processing nodes which are entangled through an on-chip quantum bus. Currently, the most promising means for realising this bus at room temperature is through dipolar coupling of adjacent NV^- electronic spins [17]. Constructing a scalable quantum device in this manner will require unprecedented control over NV fabrication at the atomic scale. For example, consider the idealised device architecture in figure 1. It features a homogeneous array of aligned NV centres which form a 2D layer of qubits. We estimate that adjacent NV^- centres must be separated by a distance of 5–10 nm for practical implementation of quantum computing. This distance regime produces a dipolar coupling between adjacent NV centres which is strong enough to achieve fast two-qubit gate operations, whilst simultaneously maintaining high stability of the NV centres' negative charge states [18].

Additionally, we estimate that a placement accuracy of ± 1 nm is required for practical implementation of quantum control at scale. Firstly, disorder in the position of each NV centre produces disorder in the coupling strength between NV centres. This can cause control errors during two-qubit gate operations. Secondly, selective control of each NV centre requires a means to differentiate their electron spin resonances using microwave pulses. This is commonly achieved through a gradient magnetic field which precisely adjusts each NV centre's resonance [19]. Hence, inaccuracies in the NV placement produces disorder in this magnetic interaction. Recent findings indicate that a placement accuracy of ± 1 nm would provide reliable spectral differentiation of NV centres and minimise disorder in their dipolar coupling [18]. Finally, each NV must be positioned relative to charged surface contacts, microwave lines, and an optical interface for qubit initialisation, readout, and control. Note that an atom-scale fabrication technique would also enable construction of alternative quantum bus architectures, for example entanglement using a chain of substitutional nitrogen atoms (N_s) [20].

The performance of quantum sensors could also be enhanced through an atom-scale fabrication technique. The next generation of NV-based magnetometers have unprecedented applications in high precision macrosensing (e.g. navigation and spatial mapping) and nanosensing (e.g. chemical analysis and nanoscopy of magnetic materials) [21, 22]. However, these capabilities cannot be fully realised at current device sensitivities, which are limited by magnetic noise from paramagnetic defects produced as a by-product of ensemble generation, low NV densities, difficulties fabricating near-surface NV centres, and inhomogeneities in NV properties such as alignment [21, 23]. Note that depending on the application, NV alignment may not be desirable such as in vector magnetometry. Similar to the quantum computing architecture, an atom-scale fabrication process can overcome these limitations through scalable production of a homogeneous array of identical NV centres in a low noise environment. Entanglement of adjacent NV^- spins is undesirable for conventional sensing, and therefore the optimum separation distance should be large enough to minimise dipolar coupling ($\gtrsim$30 nm). Conversely, previous work has demonstrated entanglement-enhanced sensitivity using quantum memory to extend coherence times, and hence smaller separations may also be desirable [24].

Existing top-down fabrication techniques face fundamental challenges in realising these stringent design requirements at scale. The current workhorse for NV fabrication with nanoscale precision is ion implantation followed by thermal annealing [25]. While this method has been highly successfully for

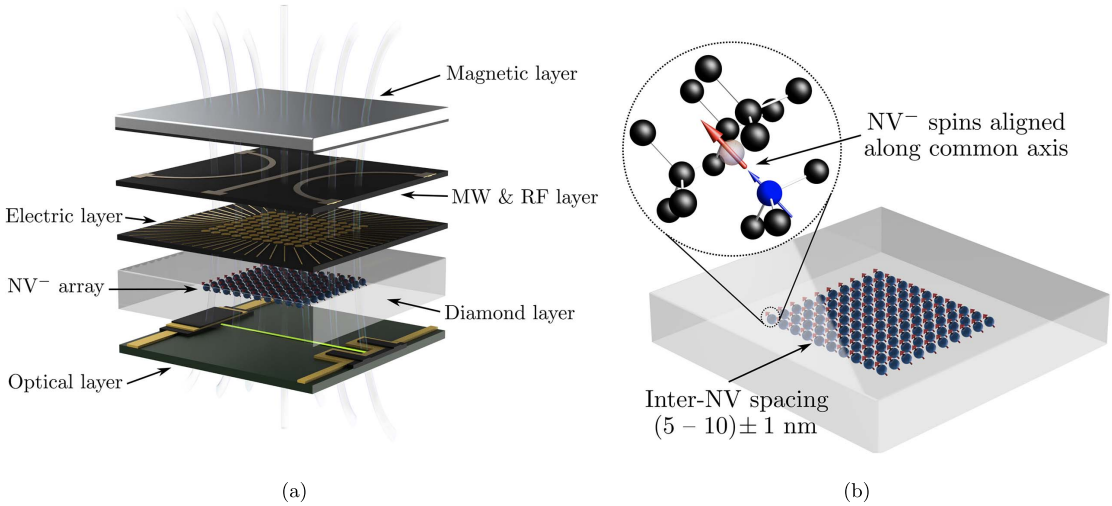

Figure 1. Idealised architecture for a scalable diamond quantum computer. This device could be realised through a bottom-up fabrication technique for NV centres, thereby enabling large-scale quantum information processing at room-temperature. (a) The integrated diamond chip consisting of a series of functional layers. A homogeneous array of NV^- centres is embedded in an ultra-pure diamond substrate (less than 1 ppb paramagnetic defects and low strain). High-fidelity initialisation and readout is performed optically and electrically via nanoscale surface contacts positioned above each individual NV centre. Quantum control is implemented through a microwave structure. (b) Zoomed-in view of the diamond layer. The NV^- centre consists of a substitutional N defect (blue sphere) adjacent to a vacant site (transparent sphere). Carbon atoms are depicted as black spheres. Each NV^- centre has uniform electronic spin properties (represented by the red arrow) and are aligned along a common axis with the same orientation. Each NV^- centre mediates initialisation, readout, and control of a spin qubit. This is the nuclear spin of the substitutional N which composes the NV centre itself (depicted by the blue arrow). Entanglement between adjacent qubits is realised through dipolar coupling of the NV^- electron spins. For room-temperature operation, this requires that neighbouring NV centres are separated by approximately 5–10 nm. Furthermore, optimal device performance requires homogeneity in this separation distance to ± 1 nm. Reproduced from [32].

fabricating NV ensembles, the stochastic nature of ion implantation severely limits its viability for fabricating next-generation devices. Firstly, there is no capability to align NV centres. Secondly, the spatial precision of implanted defects is ultimately limited by ion straggling and channelling [26]. Thirdly, there is low reproducibility in the number of implanted defects and the N-to-NV conversion yield is typically poor [25, 26]. Implantation therefore produces undesired magnetic noise which limits the performance of both quantum computers and sensors [27]. Ongoing research seeks to alleviate these limitations through several fronts, including the pursuit of deterministic single-ion implantation [28], high-resolution implantation through masks or scanning probes, and defect reduction through controlled doping [25]. Consequently, while there is considerable merit in pursuing ion implantation, it remains questionable whether the ultimate limits of the technology can meet the demands for scalable NV fabrication.

Instead, the manufacture of scalable diamond quantum devices demands a bottom-up fabrication technique which is deterministic, possesses sub-nanometre spatial precision, and preserves the purity of the crystal environment. Despite the highly demanding nature of these specifications, they are routinely achieved through hydrogen desorption lithography (HDL)-based fabrication of phosphorous defects in silicon (Si)-based quantum technologies [13]. The centrepiece of this technique is a scanning tunnelling microscope (STM) operated in both a conventional imaging mode and non-conventional desorption mode. The former is used for visualising the surface and as a critical diagnostic tool, whereas the latter enables targeted removal of hydrogen (H) termination from the Si surface with atomic-scale spatial precision [29].

Broadly speaking, the bottom-up fabrication process on Si consists of three steps. Firstly, several adjacent H atoms are desorbed to produce an active adsorption site. This consists of a chemically reactive patch of de-passivated Si surface atoms. Secondly, the surface is exposed to phosphine gas, which selectively chemisorbs to the patch but not the surrounding H resist. Thirdly, the decorated Si surface is overgrown using molecular beam homo-epitaxy to yield a bulk P defect. Importantly, no diffusion occurs during the overgrowth process, and hence the position of the incorporated defect remains unchanged from the original adsorption site. Through the de-passivation of multiple different sites in the first step, it is then possible to incorporate an entire array of P defects concurrently [30]. As this method has already been translated to germanium surfaces [31], it is likely that an analogous technique could be adapted for NV centres in diamond.

Consequently, in this perspective we outline a similar multi-step procedure for HDL-based bottom-up fabrication of NV centres. The proposed method can be implemented using existing experimental apparatus operating in non-conventional regimes. For each step, the critical requirements and open questions are

briefly summarised in light of the current state of the art and literature. It is our contention that while HDL-based fabrication of NV centres requires significant engineering, there are no fundamental impediments to its feasibility.

1. Bottom-up fabrication design

The multi-step proposal for atom-scale fabrication of NV centres is summarised in figure 2. The platform for fabrication is a high-quality mono-crystalline substrate with a (100) or (111) surface geometry. Firstly, the diamond substrate and surface is prepared for compatibility with later fabrication steps. This includes dopant incorporation for electrical conduction during STM operation, and the creation of large, atomically-flat plateaus with pristine H termination for the lithographic process [33]. Secondly, conventional STM imaging is used to identify a suitable site for molecular chemisorption. This is then followed by the creation of active adsorption sites using HDL. These sites consist of a chemically-reactive patch of de-passivated surface carbon (C) atoms which can be positioned with atomic-scale precision. Currently, STM-based lithography is the most established technique for fabricating these adsorption sites. It will therefore be the focus of this design proposal. However, we note that extreme ultraviolet (EUV)-induced desorption has recently emerged as a viable alternative to STM and may be more conducive to large-area lithography and fabrication [34].

Thirdly, the surface is exposed to a N-containing precursor gas. The molecular composition of the gas is chosen to selectively chemisorb to the reactive sites while remaining unreactive to the surrounding H termination. Fourthly, the adsorption products are verified through STM imaging. Fifthly, the surface is overgrown using chemical vapour deposition (CVD) to incorporate the adsorbed N into the diamond lattice as an NV centre. As discussed later, this may require a pre-growth stage to enhance NV yield. Following successful incorporation, the NV centre is integrated into the diamond quantum device through fabrication of an electrical, magnetic, and optical interface. This may also include further surface preparation (such as re-termination) to protect the NV centres' coherence properties and negative charge state [35].

We note that in the event of N_s incorporation instead of an NV centre during step 5, controlled vacancy production (e.g. through C-ion irradiation) and subsequent annealing to form an NV centre is a meaningful addition for the design of high-precision quantum sensors. However, this strategy is not expected to guarantee NV alignment and is therefore not viable for fabricating quantum processors.

While the qubit density can be further increased through a cluster of ^{13}C nuclei local to each NV centre, this is not essential for realising a large-scale device. Each NV centre hosts one qubit provided by its N nuclear spin, and hence scalability can be achieved without additional satellite spins. The inclusion of ^{13}C is therefore not considered in this perspective paper. However, the atom-scale fabrication process can be suitably adapted to introduce additional satellite spins if desired. For example, ^{13}C nuclei can be strategically positioned relative to each NV centre through isotopic engineering of the precursor gas.

2. Multi-step fabrication technique

Diamond preparation: Correct preparation of the diamond sample and surface is paramount before beginning the process of atom-scale fabrication. Firstly, magnetic noise degrades the NV^- coherence time and hence the performance for computing and sensing. The NV^- centres must therefore be fabricated in an ultra-pure crystal environment with negligible concentration of paramagnetic defects ($\lesssim$1 ppb) and low strain. Diamond substrates of this quality are grown commercially using CVD. However, these are also electrically insulating under ultra-high vacuum (UHV) conditions and therefore incompatible with conventional STM imaging and HDL. Consequently, electrical conductivity must be introduced into the sample while simultaneously maintaining a low-noise environment local to the NV^- centres.

Conductivity in diamond is typically realised through thermal activation of boron dopants, which can be introduced at high densities and spatial precision through ion implantation. Unfortunately, boron dopants are also paramagnetic and will decohere nearby NV^- centres. We therefore envisage the fabrication of doped regions at a distance from an intrinsic region which hosts the NV centres. By optimising the separation distance (estimated on the scale of hundreds of nanometres), carriers could be drawn from the dopant layer to enable conductivity during imaging/lithography while mitigating unwanted magnetic noise in the final device. Such device designs have been extensively studied in the context of diamond junctions [36], but not yet adapted for STM.

Although B doping in diamond is now technologically mature, *p*-type conductivity is undesirable in NV-based technologies because valence holes cause deleterious bleaching of the negative charge state [37]. The preferred option is *n*-type doping using phosphorous defects which are still paramagnetic but serve to stabilise NV^-. As with boron doping, phosphorous defects can be implanted at a distance from the intrinsic region which hosts the NV centres. However, further development of phosphorus doping is required to

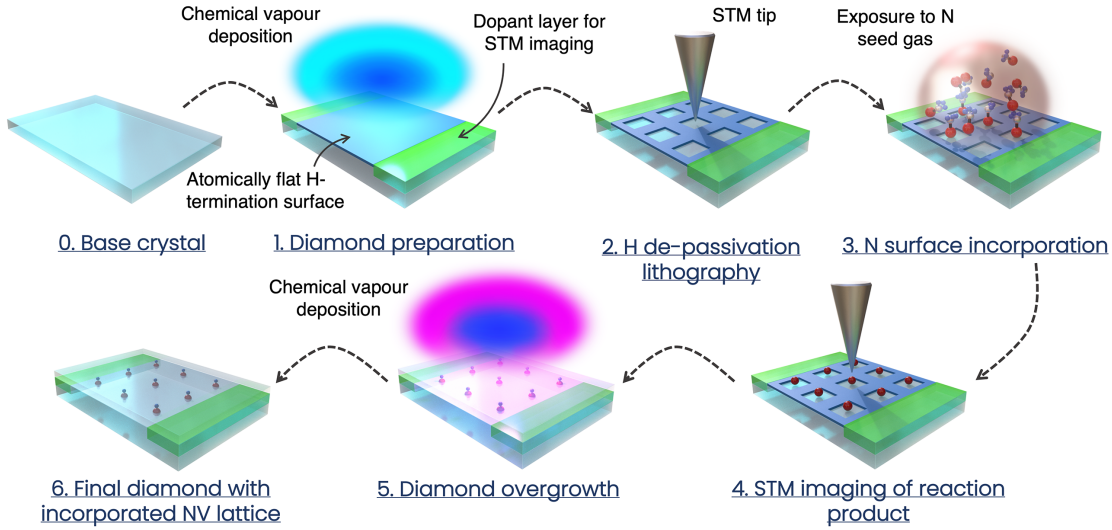

Figure 2. Atom-scale fabrication of scalable diamond quantum devices. 0. The platform for fabrication is a mono-crystalline (100) or (111) diamond substrate. 1. The substrate is prepared for fabrication. This entails ultra-pure CVD overgrowth of an intrinsic diamond layer. The ideal surface is H-terminated with a low concentration of defects and low surface roughness. Additionally, ion implantation is used to produce doped regions distant from the intrinsic fabrication region. These doped regions provide bulk conductivity which is critical for performing STM under UHV conditions. 2. An array of active sites is fabricated with atomic-scale precision through STM-based HDL. These sites are chemically reactive patches of de-passivated surface C atoms. They possess a high density of dangling bonds which facilitate molecular chemisorption. 3. The surface is exposed to a N-based precursor gas which preferentially adsorbs to the active sites. The surrounding H termination acts as a molecular resist. 4. Adsorption of N is confirmed and analysed through conventional STM imaging. 5. The sample is relocated to a CVD chamber for ultra-pure diamond overgrowth. The N adsorbates are incorporated into the diamond lattice to form bulk NV centres. 6. The NV centres can now be integrated into the diamond quantum device through fabrication of an electrical, magnetic, and optical interface.

achieve adequate conductivity at STM-compatible temperatures. For example, the reduction of compensation ratios through improved doping techniques [38, 39]. Alternatively, STM imaging on purely insulating samples is possible through an unconventional high-bias resonant tunnelling regime [40].

Regarding surface preparation, the H-terminated (100) and (111) facets are currently the most viable for atom-scale fabrication. The (111) facet has several superior qualities compared to (100), chiefly the preferential alignment of as-grown NV centres [41]. The ideal properties for both surfaces include low roughness, with atomically-flat terraces large enough for practical implementation of HDL and subsequent molecular chemisorption (on the scale of several nm^2). It may also be beneficial for surfaces to possess a small miscut angle to enhance the NV incorporation yield. For example, experimental studies find that the incorporation of other dopants increases with step-edge density [42–44].

Reproducible fabrication of high-quality diamond surfaces presents a surmountable engineering challenge. Existing surface preparation protocols, including a combination of CVD overgrowth, mechanical polishing, cleaning, and re-passivation using H plasma, must be adapted for consistency of quality and scale. Obtaining high-quality (111) surfaces is particularly challenging due to a larger density of as-grown defects, obstacles associated with mechanical polishing, and the optimisation of CVD growth parameters. However, there are no fundamental barriers to such surface preparation as evidenced by several works demonstrating atomically-flat (111) surfaces [45–47]. As an additional example, figure 3(e) displays an STM image of a high-quality H-terminated (111) surface produced by Quantum Brilliance. The surface possesses large and atomically-flat regions (on the scale of μm^2) which are suitable for atom-scale fabrication.

HDL: HDL is a surface patterning technique developed over the last three decades on semiconductor surfaces, in particular Si [29, 48]. It entails the targeted removal of H termination to form chemically-reactive patches of de-passivated C atoms on the diamond surface. Subsequently, these exposed C sites provide anchor points for molecular adsorbates. Key considerations for developing room-temperature quantum devices are the chemical reactivity of the patch to chemisorption, optimising the patch dimensions such that only a single N may chemisorb per site (multiple N adsorbates per site are generally undesirable), and the spatial positioning of the fabricated NV centres. As previously noted, the lateral spacing between adjacent NV centres must be accurate to within ± 1 nm to maintain optimal dipolar interactions whilst avoiding undesirable coupling disorder.

Presently, STM is the workhorse to perform at this level of spatial precision. Implementation of HDL requires the use of conventional STM imaging followed by an unconventional desorption mode. Both must

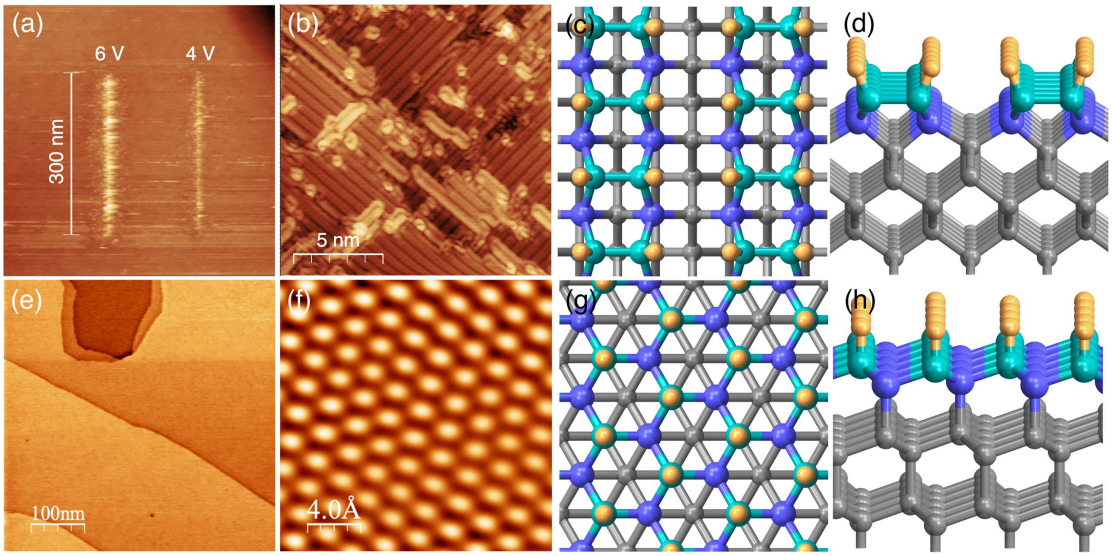

Figure 3. Imaging, visualisation, and manipulation of diamond surfaces. (a) Constant current STM image (−1.5 V, 0.2 nA) demonstrating tip-based manipulation of the H–C(100):2 × 1 surface. The STM tip has been dragged along a line during voltage pulsing at 4 V and 6 V. This produces bright features which indicate surface manipulation including possible H desorption. (b) Zoomed-in STM image of the H–C(100):2 × 1 surface displaying the characteristic dimer rows of the 2 × 1 reconstruction (−1.5 V, 1 nA). (c),(d) Visualisation of the H–C(100):2 × 1 surface geometry. The surface C atoms (cyan) form characteristic dimer rows terminated by H atoms (orange). The second layer of C atoms have been highlighted in blue, whereas deeper subsurface C atoms are grey. (e) Constant current STM image of a H–C(111):1 × 1 surface (−1 V, 0.2 nA). This wide-area scan displays atomically-flat regions with areas on the scale of μm^2. The different regions are separated by step edges. (f) Zoomed-in STM image of the H–C(111):1 × 1 surface which displays an atomically-resolved hexagonal lattice (1.4 V, 1 nA). Note that FFT filtering of the topography has been applied to reduce high-frequency spatial noise. (g),(h) Visualisation of the H–C(111):1 × 1 surface geometry displaying a characteristic hexagonal structure. The colour scheme is the same as (c).

be performed under UHV conditions. Imaging is necessary to identify a suitable adsorption site prior to lithography. Ideally, this is an atomically-flat plateau which is sufficiently large to accommodate the molecular adsorbate ($\gtrsim$1 nm^2). Although STM imaging of diamond surfaces is generally considered difficult, it is routinely performed with conventional STM apparatus and enabled by *p*-type conductivity through boron doping (see figure 3). Following imaging, targeted H desorption is realised through an inelastic tunnelling mode. In this low voltage process, the C–H stretch mode is excited resonantly to induce bond-breaking via the coupling between tunnelling electrons and local vibration modes [49]. Extrapolating known results on Si, maintaining a voltage below the field emission regime is essential to maximising spatial resolution of the lithographed region [50].

The capabilities of lithography on diamond are promising but underdeveloped. While Si HDL is now a mature technique capable of near-deterministic removal of single H atoms [29], attention to diamond has been sparse in the literature. Notably, a remarkable demonstration of feasibility has been achieved by Bobrov and collaborators on diamond (100) surfaces [51]. Hydrogen desorption was achieved through application of controlled voltage pulses. This produced bright features in the STM topography which were subsequently identified as de-passivated surface C atoms using scanning tunnelling spectroscopy. However, the demonstrated spatial precision was limited, with desorption events occurring within several nanometres of the target C–H bond.

Quantum Brilliance has recently replicated the voltage pulsing technique to manipulate the diamond (100) surface. Figure 3(a) presents an STM topography following application of voltage pulses along a straight line. This produced bright features qualitatively similar to those observed in Bobrov *et al*'s work, and are hypothesised to represent surface defects including de-passivated C atoms. Ultimately, further work is needed to verify the defect chemical structure, improve the control of the lithographic process, and extend these capabilities to other surfaces such as (111).

Another key challenge lies with the surface reconstruction of de-passivated patches following HDL. Ideally, lithography produces a patch of highly-reactive C surface radicals, termed *dangling bonds*, which facilitate molecular chemisorption at low temperatures and pressures. However, these dangling bonds can self-passivate through surface reconstruction, thereby drastically reducing the chemical reactivity of the patch. This could render chemisorption of the N-based molecule energetically unfavourable or require temperatures and pressures which are practically unachievable (as defined in the following section). For example, the H-terminated (100) surface possesses characteristic CH–CH dimer rows which are visible in

figures 3(b)–(d). Each dimer contains a pair of σ-bonded surface C atoms, both of which are terminated with a H atom. Desorption of a single H atom in a given dimer produces a reactive dangling bond localised on one of the C sites. However, desorption of both H atoms causes the dangling bonds on the C atoms to self-passivate through formation of a π bond [52, 53]. The resulting C–C dimer is termed as 'bare', and exhibits substantially less reactivity to molecular chemisorption as discussed in more detail below [54].

Surface reconstruction on the (111) surface is substantially more complex. If the H-terminated surface is fully de-passivated (e.g. through thermal annealing at temperatures greater than 1200 K [55]), the surface C atoms will reconstruct to form π-bonded Pandey chains. Unfortunately, these chains exhibit limited reactivity to molecular chemisorption [52, 56, 57]. A similar reconstruction would be undesirable on the lithographed patches, but the critical patch size required for this reconstruction to occur is currently unknown. For example, desorption of a single H atom produces a reactive dangling bond. However, desorption of a larger patch through HDL may induce local surface reconstruction to form chemically-inert Pandey chains. This further motivates development of a lithographic technique with the highest possible spatial resolution, ideally approaching the ultimate precision—deterministic removal of single H atoms.

Molecular chemisorption: The third step in the atom-scale fabrication process is chemisorption of N onto the de-passivated patches produced using HDL. Although diamond is typically considered an inert material, a diverse array of techniques exist for the chemical modification of its surface with N-containing species [58]. Unfortunately, established methods such as plasma treatment or photochemical functionalisation are much too volatile and would invariably result in unwanted chemsiorption outside the lithographed region. The successful chemisorption process must therefore balance reactivity with the de-passivated sites without destroying the surrounding H resist. While thermal control can direct this balance, the temperature cannot exceed the desorption temperature of the H termination (approximately 1200 K [55, 59]). This implies that practical reactions will be thermally-assisted chemisorption of neutrally charged and non-radical molecules. Realistically, this precursor gas would be introduced *in situ* into the STM chamber post lithography.

The structure and chemistry of the adsorption site is paramount when evaluating candidate molecules for chemisorption. Although dangling bonds are desirable for surface reactivity, other forms of chemisorption appear to be possible on bare (100) dimers and Pandey chains. Experimental work on the clean (100) surface suggests that alkenes and alkynes can adsorb via cycloaddition with π bonds of the C=C dimer rows. For example, low reactivity is found with cyclopentene, 1,3-butadiene, allyl alcohol, acrylic acid, allyl chloride [60], and notably acrylonitrile which contains a cyanide group [61]. Beyond these examples, substantial reactivity with other small organic molecules has yet to be identified. While phosphine readily adsorbs to the buckled dimers of Si(100), the molecular analogue for diamond, ammonia, does not appear to adsorb to the symmetric C(100) dimers, nor the cleanly-terminated (111) or (110) surfaces [62]. The same holds for nitrogen gas, N_2. In general, thermally-driven chemisorption on the (111) surface has received little experimental attention [57].

There are three simple heuristics which can guide the selection of candidate molecules for chemisorption. Firstly, the molecule ought to consist only of C, H, and a single N atom as to avoid incorporation of undesired defects and impurities during subsequent diamond overgrowth. Secondly, the adsorbate must be extremely stable in order to withstand desorption or migration during CVD overgrowth. Finally, during overgrowth the adsorbed N should preferentially incorporate as an NV centre with well-defined orientation. First-principles calculations offer an efficient method for screening candidate molecules according to these heuristics and is the subject of current and future work.

Potential molecules may include those with adsorbate structures that are compatible with overgrowth. This is because adsorbates with a similar geometry to natural growth structures could be more resistant to desorption during CVD. For example, nitriles possess a $-C{\equiv}N$ functional group which has a bond length comparable to the distance between C atoms on the (100) surface. If the nitrile chemisorbs along the dimer row (forming an imine ($-C{=}N-$) bridge between two adjacent surface C atoms), the resulting adsorbate resembles those occurring in new-layer nucleation [63]. Aromatic N heterocycles could be viable on the (111) surface. For example, pyridine and indolizine possess similar geometries to the surface C atoms. Covalent bonding between the molecules' C atoms and the diamond surface could produce a structure resembling the subsequent growth layer [64].

Overgrowth, incorporation, and NV formation: The final stage of the atom-scale fabrication process involves incorporation of the N adsorbate into the diamond structure to form a bulk NV centre. This is a key challenge which necessitates overgrowth of the decorated surface while simultaneously maintaining high NV yields. While formation of single crystals is possible through high-pressure-high-temperature growth methods, CVD is the only method capable of reliable homo-epitaxial diamond overgrowth with low defect concentrations. The volatility of the standard CVD growth environment—including substrate temperatures up to 1100 K and H fluxes reaching 10^{23} $cm^{-2}s^{-1}$—has great potential for N desorption or surface migration

[65]. Despite this, recent research suggests that N adsorbates are capable of withstanding both high temperatures and H flux, and incorporate with low but promising yields during CVD overgrowth [66, 67].

Perhaps most relevant to atom-scale fabrication is the N retention rate following diamond overgrowth. This has been the focus of several experimental studies involving a pre-growth N-based plasma treatment to partially terminate the diamond surface with N adsorbates. Using a combination of measurement techniques, the pre-growth N surface concentration is compared to the post-growth density of bulk N defects and NV centres. For example, Kuntumalla *et al* considered (100) surfaces terminated using a variety of N-based plasma treatments and overgrown using conventional CVD [66]. Depending on the type of plasma treatment (and therefore the bonding chemistry of the N adsorbates with the surface), between 5% and 34% of the N termination was retained and incorporated into the bulk diamond crystal. A similar study was recently performed by Tatsuishi *et al* [67] on the (111) surface, which revealed N retention rates of approximately 2.5%.

These promising results indicate that N incorporation is possible despite the volatility of the CVD plasma environment. Moreover, there exist multiple avenues for increasing N retention. Firstly, as demonstrated by Kuntumalla *et al*'s study, the retention rate is critically determined by the bonding configuration of the N adsorbate [66]. Maximising retention therefore requires engineering the adsorption reaction through considered choice of the N-containing molecule in the precursor gas and design of the adsorption site. Secondly, it may also be possible to further protect the N adsorbate from the CVD environment through depositing a protective C layer prior to overgrowth.

Beyond N retention, a further challenge lies in maximising the N-to-NV conversion yield during overgrowth. Currently, the formation of as-grown NV centres is a stochastic process, and little research has focused on improving efficiency in a controlled manner. In addition to optimising the CVD reactor conditions, we propose that the adsorbate chemistry is key to promoting V formation. Recall that the N adsorbate ideally forms an as-grown NV centre, and that a major benefit of the (111) surface is that as-grown NV centres are aligned predominately along the [111] axis (i.e. the growth direction)[41]. First-principles studies suggest that this alignment is due to the chemical stability of the N lone pair [68, 69]. Nitrogen atoms at the (111) surface resist forming bonds with other C atoms during overgrowth of the next layer, thereby producing an adjacent vacancy and subsequent NV centre. Hence, one pathway to deterministic NV formation may be to replicate this bonding environment in the N adsorbate. This would require engineering the adsorption chemistry such that the N lone pair aligns with the [111] axis. However, further experimentation is required to validate the feasibility of this approach.

3. Conclusion

Realising the ultimate potential of diamond quantum technologies will require development of a bottom-up NV fabrication technique which is scalable, deterministic, and possesses nanoscale spatial precision. In this perspective article we have outlined a method for atomically-precise manufacturing of NV centres using HDL. The efficacy of similar techniques has already been demonstrated on silicon and germanium, and we believe that there are no fundamental reasons why these cannot be adapted to diamond.

Success will require experimental and theoretical progress on several fronts. For example, diamond HDL must achieve higher spatial accuracy (ideally reaching single-site precision), a suitable N-based molecule must be identified and its adsorption chemistry optimised, and the rates of N retention and N-to-NV conversion during overgrowth must be improved. Hence, while bottom-up fabrication on diamond surfaces presents significant engineering and technical challenges, these are quantifiable and can be overcome through sustained community effort. Recent progress in the fields of nano-electronics, NV physics, atomic-scale microscopy and C deposition techniques all provide a timely opportunity for cross-discipline collaboration. We therefore anticipate and welcome forthcoming developments in the burgeoning field of atom-scale NV fabrication.

Data availability statement

All data that support the findings of this study are included within the article (and any supplementary files).

Acknowledgments

This research was supported by the Australian Government through the Australian Research Council's Linkage Projects funding scheme (Poject LP200301428). This work was performed in part at the Melbourne Centre for Nanofabrication (MCN) in the Victorian Node of the Australian National Fabrication Facility (ANFF).

ORCID iDs

Lachlan Oberg https://orcid.org/0000-0002-4560-1833
Cedric Weber https://orcid.org/0000-0002-6989-2700
Hung-Hsiang Yang https://orcid.org/0000-0002-9592-4155
Philipp Reinke https://orcid.org/0000-0002-3644-2738
Santiago Corujeira Gallo https://orcid.org/0000-0002-7305-2931
Alastair Stacey https://orcid.org/0000-0002-3794-0317
Christopher I Pakes https://orcid.org/0000-0003-3986-0780
Marcus W Doherty https://orcid.org/0000-0002-5473-6481

References

[1] Doherty M W, Manson N B, Delaney P, Jelezko F, Wrachtrup J and Hollenberg L C L 2013 The nitrogen-vacancy colour centre in diamond *Phys. Rep.* **528** 1–45
[2] Rong X, Geng J, Shi F, Liu Y, Kebiao X, Wenchao M, Kong F, Jiang Z, Yang W and Jiangfeng D 2015 Experimental fault-tolerant universal quantum gates with solid-state spins under ambient conditions *Nat. Commun.* **6** 8748
[3] Pezzagna S and Meijer J 2021 Quantum computer based on color centers in diamond *Appl. Phys. Rev.* **8** 011308
[4] Hong S, Grinolds M S, Pham L M, Sage D L, Luan L, Walsworth R L and Yacoby A 2013 Nanoscale magnetometry with NV centers in diamond *MRS Bull.* **38** 155–61
[5] Pang Y Y, Leung W K, Zhao N, Ho K O, Yang Shen and Sen Yang 2021 Diamond quantum sensors: from physics to applications on condensed matter research *Funct. Diam.* **1** 160–173
[6] Doherty M 2021 Quantum accelerators: a new trajectory of quantum computers *Digit. Welt* **5** 74–79
[7] Humble T S, McCaskey A, Lyakh D I, Gowrishankar M, Frisch A and Monz T 2021 Quantum computers for high-performance computing *IEEE Micro* **41** 15–23
[8] Weitang Li *et al* 2024 A hybrid quantum computing pipeline for real world drug discovery *Sci. Rep.* **14** 16942
[9] Rossmannek M, Panagiotis K Barkoutsos P J O and Tavernelli I 2021 Quantum HF/DFT-embedding algorithms for electronic structure calculations: scaling up to complex molecular systems *J. Chem. Phys.* **154** 114105
[10] Bausch J, Subramanian S and Piddock S 2021 A quantum search decoder for natural language processing *Quantum Mach. Intell.* **3** 16
[11] Yoshinaga A, Tatsuta M and Matsuzaki Y 2021 Entanglement-enhanced sensing using a chain of qubits with always-on nearest-neighbor interactions *Phys. Rev. A* **103** 062602
[12] Simmons M Y, Schofield S R, O'Brien J L, Curson N J, Lars Oberbeck T H and Clark R G 2003 Towards the atomic-scale fabrication of a silicon-based solid state quantum computer *Surf. Sci.* **532-535** 1209–18
[13] Fuechsle M, Miwa J A, Mahapatra S, Ryu H, Lee S, Warschkow O, Hollenberg L C L, Klimeck G and Simmons M Y 2012 A single-atom transistor *Nat. Nanotechnol.* **7** 242–6
[14] Waldherr G *et al* 2014 Quantum error correction in a solid-state hybrid spin register *Nature* **506** 204–7
[15] Taminiau T H, Cramer J, van der Sar T, Dobrovitski V V and Hanson R 2014 universal control and error correction in multi-qubit spin registers in diamond *Nat. Nanotechnol.* **9** 171–6
[16] Bradley C E, Randall J, Abobeih M H, Berrevoets R C, Degen M J, Bakker M A, Markham M, Twitchen D J and Taminiau T H 2019 A ten-qubit solid-state spin register with quantum memory up to one minute *Phys. Rev. X* **9** 031045
[17] Wenzheng Dong F A C-V and Economou S E 2020 Precise high-fidelity electron–nuclear spin entangling gates in NV centers via hybrid dynamical decoupling sequences *New J. Phys.* **22** 073059
[18] Chen Y 2024 Optimisation and scaling of diamond quantum computers *PhD Thesis* Department of Quantum Science & Technology, The Australian National University
[19] Zhang H, Arai K, Belthangady C, Jaskula J-C and Walsworth R L 2017 Selective addressing of solid-state spins at the nanoscale via magnetic resonance frequency encoding *npj Quantum Inf.* **3** 31
[20] Yao N Y, Jiang L, Gorshkov A V, Maurer P C, Giedke G, Cirac J I and Lukin M D 2012 Scalable architecture for a room temperature solid-state quantum information processor *Nat. Commun.* **3** 800
[21] Rondin L, Tetienne J-P, Hingant T, Roch J-F, Maletinsky P and Jacques V 2014 Magnetometry with nitrogen-vacancy defects in diamond *Rep. Prog. Phys.* **77** 056503
[22] Degen C L, Reinhard F and Cappellaro P 2017 Quantum sensing *Rev. Mod. Phys.* **89** 035002
[23] Barry J F, Schloss J M, Bauch E, Turner M J, Hart C A, Pham L M and Walsworth R L 2020 Sensitivity optimization for nv-diamond magnetometry *Rev. Mod. Phys.* **92** 015004
[24] Zaiser S, Rendler T, Jakobi I, Wolf T, Lee S-Y, Wagner S, Bergholm V, Schulte-Herbrüggen T, Neumann P and Wrachtrup J 2016 Enhancing quantum sensing sensitivity by a quantum memory *Nat. Commun.* **7** 12279
[25] Lühmann T, Meijer J and Pezzagna S 2021 Charge-assisted engineering of color centers in diamond *Phys. Status Solidi a* **218** 2000614
[26] Pezzagna S, Naydenov B, Jelezko F, Wrachtrup J and Meijer J 2010 Creation efficiency of nitrogen-vacancy centres in diamond *New J. Phys.* **12** 065017
[27] Taylor J M, Cappellaro P, Childress L, Jiang L, Budker D, Hemmer P R, Yacoby A, Walsworth R and Lukin M D 2008 High-sensitivity diamond magnetometer with nanoscale resolution *Nat. Phys.* **4** 810–6
[28] Jakob A M *et al* 2022 Deterministic shallow dopant implantation in silicon with detection confidence upper-bound to 99.85% by ion-solid interactions *Adv. Mater.* **34** 2103235
[29] Alemansour H, Reza Moheimani S O, Owen J H G, Randall J N and Fuchs E 2020 Controlled removal of hydrogen atoms from H-terminated silicon surfaces *J. Vac. Sci. Technol. B* **38** 040601
[30] Kiczynski M, Gorman S K, Geng H, Donnelly M B, Chung Y, He Y, Keizer J G and Simmons M Y 2022 Engineering topological states in atom-based semiconductor quantum dots *Nature* **606** 694–9
[31] Scappucci G, Capellini G, Johnston B, Klesse W M, Miwa J A and Simmons M Y 2011 A complete fabrication route for atomic-scale, donor-based devices in single-crystal germanium *Nano Lett.* **11** 2272–9 (PMID: 21553900)

[32] Oberg L 2024 Atom-scale fabrication and applications of diamond quantum devices *PhD Thesis* Department of Quantum Science & Technology, The Australian National University
[33] McCloskey D J, Roberts D, Rodgers L V H, Barsukov Y, Kaganovich I D, Simpson D A, de Leon N P, Stacey A and Dontschuk N 2024 Methods for color center preserving hydrogen-termination of diamond *Adv. Mater. Interfaces* **11** 2400242
[34] Constantinou P, Stock T J Z, Tseng Li-T, Kazazis D, Muntwiler M, Vaz C A F, Ekinci Y, Aeppli G, Curson N J and Schofield S R 2024 EUV-induced hydrogen desorption as a step towards large-scale silicon quantum device patterning *Nat. Commun.* **15** 694
[35] Kaviani M, Deák P, Aradi B, Frauenheim T, Chou J-P and Gali A 2014 Proper surface termination for luminescent near-surface NV centers in diamond *Nano Lett.* **14** 4772–7
[36] Haruyama M *et al* 2023 Electroluminescence of negatively charged single NV centers in diamond *Appl. Phys. Lett.* **122** 072101
[37] Lozovoi A, Jayakumar H, Daw D, Vizkelethy G, Bielejec E, Doherty M W, Flick J and Meriles C A 2021 Optical activation and detection of charge transport between individual colour centres in diamond *Nat. Electron.* **4** 717–24
[38] Stenger I, Pinault-Thaury M-A, Temahuki N, Gillet R, Temgoua S, Bensalah H, Chikoidze E, Dumont Y and Barjon J 2021 Electron mobility in (100) homoepitaxial layers of phosphorus-doped diamond *J. Appl. Phys.* **129** 105701
[39] Pinault-Thaury M-A, Stenger I, Gillet R, Temgoua S, Chikoidze E, Dumont Y, Jomard F, Kociniewski T and Barjon J 2021 Attractive electron mobility in (113) N-type phosphorus-doped homoepitaxial diamond *Carbon* **175** 254–8
[40] Bobrov K, Mayne A J and Dujardin G 2001 Atomic-scale imaging of insulating diamond through resonant electron injection *Nature* **413** 616–9
[41] Michl J *et al* 2014 Perfect alignment and preferential orientation of nitrogen-vacancy centers during chemical vapor deposition diamond growth on (111) surfaces *Appl. Phys. Lett.* **104** 102407
[42] Pinault-Thaury M-A, Tillocher T, Kobor D, Habka N, Jomard F, Chevallier J and Barjon J 2011 Phosphorus donor incorporation in (100) homoepitaxial diamond: role of the lateral growth *J. Cryst. Growth* **335** 31–36
[43] Meynell S A, McLellan C A, Hughes L B, Wang W, Mates T E, Mukherjee K and Jayich A C B 2020 Engineering quantum-coherent defects: the role of substrate miscut in chemical vapor deposition diamond growth *Appl. Phys. Lett.* **117** 194001
[44] Mortet V *et al* 2022 Effect of substrate crystalline orientation on boron-doped homoepitaxial diamond growth *Diam. Relat. Mater.* **122** 108887
[45] Tokuda N, Umezawa H, Yamabe K, Okushi H and Yamasaki S 2010 Growth of atomically step-free surface on diamond 111 mesas *Diam. Relat. Mater.* **19** 288–90
[46] Tokuda N, Makino T, Inokuma T and Yamasaki S 2012 Formation of step-free surfaces on diamond (111) mesas by homoepitaxial lateral growth *Jpn. J. Appl. Phys.* **51** 090107
[47] Yoshida R, Miyata D, Makino T, Yamasaki S and Matsumoto T 2018 Takao Inokuma and Norio Tokuda. Formation of atomically flat hydroxyl-terminated diamond (111) surfaces via water vapor annealing *Appl. Surf. Sci.* **458** 222–5
[48] Shen T C, Wang C, Abeln G C, Tucker J R, Lyding J W, vouris P and Walkup R E 1995 Atomic-scale desorption through electronic and vibrational excitation mechanisms *Science* **268** 1590–2
[49] Morgenstern K, Lorente N and Rieder K-H 2013 Controlled manipulation of single atoms and small molecules using the scanning tunnelling microscope *Phys. Status Solidi b* **250** 1671–751
[50] Randall J N, Owen J H G, Lake J, Saini R, Fuchs E, Mohammad Mahdavi S O R M and Schaefer B C 2018 Highly parallel scanning tunneling microscope based hydrogen depassivation lithography *J. Vac. Sci. Technol. B* **36** 06JL05
[51] Bobrov K, Mayne A J, Hoffman A and Dujardin G 2003 Atomic-scale desorption of hydrogen from hydrogenated diamond surfaces using the STM *Surf. Sci.* **528** 138–43
[52] Ristein J 2006 Diamond surfaces: familiar and amazing *Appl. Phys. A* **82** 377–84
[53] Gomez H, Groves M N and Neupane M R 2021 Study of the structural phase transition in diamond (100) & (111) surfaces *Carbon Trends* **3** 100033
[54] Cho J H and Kleinman L 2003 Hydrogen catalyzed adsorption of alkenes on the diamond (001) surface *Phys. Rev. B* **68** 11
[55] Su C, Song K-J, Wang Y L, Lu H-L, Chuang T J and Lin J-C 1997 Hydrogen chemisorption and thermal desorption on the diamond C(111) surface *J. Chem. Phys.* **107** 7543–58
[56] Levita G, Kajita S and Righi M C 2018 Water adsorption on diamond (111) surfaces: an AB initio study *Carbon* **127** 533–40
[57] Hoh H Y, Ouyang T, Sullivan M B, Ping W, Nesladek M and Loh K P 2010 A HREELS and DFT study of the adsorption of aromatic hydrocarbons on diamond (111) *Langmuir* **26** 3286–91
[58] Raymakers J, Haenen K and Maes W 2019 Diamond surface functionalization: from gemstone to photoelectrochemical applications *J. Mater. Chem.* **7** 10134–65
[59] Thomas R E, Rudder R A and Markunas R J 1992 Thermal desorption from hydrogenated and oxygenated diamond (100) surfaces *J. Vac. Sci. Technol. A* **10** 2451–7
[60] Ouyang T, Gao X, Dongchen Q, Wee A T S and Loh K P 2006 Cycloadditions on diamond (100) 2 × 1: observation of lowered electron affinity due to hydrocarbon adsorption *J. Phys. Chem. B* **110** 5611–20 (PMID: 16539504)
[61] Schwartz M P, Barlow D E, Russell J N, Butler J E, D'Evelyn M P and Hamers R J 2005 Adsorption of acrylonitrile on diamond and silicon (001)−(2× 1) surfaces: effects of dimer structure on reaction pathways and product distributions *J. Am. Chem. Soc.* **127** 8348–54 (PMID: 15941268)
[62] Lurie P G and Wilson J M 1977 The diamond surface: I. The structure of the clean surface and the interaction with gases and metals *Surf. Sci.* **65** 453–75
[63] Sung Y-Y *et al* 2024 Identification of defects and the origins of surface noise on hydrogen-terminated (100) diamond *Adv. Mater. Interfaces* **12** 2400695
[64] Dohery M, Oberg L, Weber C, Sergeieva T, Pakes C, Schenk A and Stacey A 2023 *Atomic Scale Fabrication of Diamond Quantum Computers, Patent, WIPO (PCT), WO2023097361*
[65] Butler J E, Mankelevich Y A, Cheesman A, Jie M and Ashfold M N R 2009 Understanding the chemical vapor deposition of diamond: recent progress *J. Phys.: Condens. Matter* **21** 364201
[66] Kuntumalla M K, Attrash M, Fischer M, Michaelson S, Kravchuk T and Hoffman A 2021 Nitrogen and hydrogen distribution and retention in dense N delta doping by layer overgrowth onto a diamond (100) surface *Appl. Surf. Sci.* **550** 149331
[67] Tatsuishi T *et al* 2021 Highly aligned 2d NV ensemble fabrication from nitrogen-terminated (111) surface *Carbon* **180** 127–34
[68] Fukui T *et al* 2014 Perfect selective alignment of nitrogen-vacancy centers in diamond *Appl. Phys. Express* **7** 055201
[69] Miyazaki T, Miyamoto Y, Makino T, Kato H, Yamasaki S, Fukui T, Doi Y, Tokuda N, Hatano M and Mizuochi N 2014 Atomistic mechanism of perfect alignment of nitrogen-vacancy centers in diamond *Appl. Phys. Lett.* **105** 261601